EXPERIMENTAL EVIDENCE FOR ION ACOUSTIC SOLITONS IN THE PLUME OF A HOLLOW CATHODE

Marcel P. Georgin[1], Benjamin A. Jorns[2], and Alec D. Gallimore[3]

[1] *Applied Physics Program, University of Michigan, Ann Arbor, MI, 48109, USA, georginm@umich.edu*
[2] *Department of Aerospace Engineering, University of Michigan, Ann Arbor, MI, 48109, USA, bjorns@umich.edu*
[3] *Department of Aerospace Engineering, University of Michigan, Ann Arbor, MI, 48109, USA, alec.gallimore@umich.edu*

KEYWORDS

Hollow cathodes, coherent plasma waves, ion acoustic turbulence

ABSTRACT

Ion saturation probes are used to characterize the propagating modes in the plume of a hollow cathode discharge. Coherent, low-frequency structures are shown to coexist with ion acoustic turbulence. The measurements show that these waves evolve in a manner that suggests that they originate from a localized disturbance in the plasma. The large-scale fluctuations and ion acoustic turbulence propagate towards the anode while a quasi-periodic wave propagates towards the cathode. The large amplitude structures are compared with a fluid formulation of weakly nonlinear ion acoustic solitons. The height-to-width ratio and velocity of the detected soliton-like structures are shown to be in good agreement with soliton theory. However, a direct estimate of the width is four orders of magnitude smaller than that measured by the probes. This discrepancy is discussed in the context of simplifications for ion soliton theory that may not be applicable to this plasma. In addition to these oscillations in density, the total energy density of the turbulent ion acoustic (IAT) modes has been observed to fluctuate at the same frequency as the oscillations in the plasma density. The turbulent energy wave propagates in the plasma with an evolving phase relationship with density oscillation. The shape of the IAT energy wave is similar to the soliton-like density structures; the waveform is also well described by a soliton profile. The estimated temporal width is equal that of the density soliton, however the amplitude of the IAT energy wave is about three times larger than the soliton. This experimental evidence suggests that the local disturbance generates IAT in the form of a wave packet. In light of these measurements and analytical theory, the following physical picture emerges from this study: a periodic, localized disturbance is established in the cathode plume and deposits energy into several modes including turbulent ion acoustic wave packets, ion acoustic solitons and quasi-periodic waves that propagate away from this region.

1 INTRODUCTION

Hollow cathodes are electron current sources that are commonly used in electric propulsion systems to provide the discharge current or neutralize ion beams. Despite decades of flight heritage, there remain two poorly understood processes that can play an important role in the transient operation of a hollow cathode that are non-classical: ion acoustic turbulence and coherent, low-frequency plasma oscillations. To date, several studies have focused on turbulent ion acoustic waves (IAT) that are present in the hollow cathode plume.[1–3] Through theory, experiments, and modeling, it has been shown that this turbulence affects the steady state electron resistivity in the cathode plume and

is necessary to develop a self-consistent numerical model of the cathode. The low-frequency plasma oscillations, on the other hand, still lack a physical understanding. These propagating structures occur in the range of 20-200 kHz, onset in hollow cathode discharges at low flow rates and high currents and generate large plasma potential fluctuations.[4–7] These plasma oscillations are often associated with the so-called hollow cathode plume mode where the erosion rate of the keeper increases by an order of magnitude. When these oscillations are empirically included into numerical models, the erosion rates are in agreement with experimental measurements.[8] Understanding the nature of these oscillations can lead to a more accurate prediction of the onset of this erosive state and may eventually lead to its control and mitigation.

Although the nature of these oscillations is unknown, there have been a number of empirical studies to characterize them. These studies have showed that the large-amplitude waves exist in the cathode plume, but not in the internal cathode plasma, suggesting that the waves form and grow solely in the plume.[9] Further investigation has shown that these structures propagate near the ion acoustic speed from the cathode towards the anode.[10] In light of these known experimental properties, there are several theories in the literature proposing a physical mechanism behind the onset of these low-frequency oscillations and the cathode plume mode.[9, 11, 12] The most common interpretation of the onset criterion is an ionization-like predator-prey oscillation.[9, 13] In this model, the electrons are the predators and the neutrals are the prey. If the current is increased sufficiently for a fixed mass flow rate, the electron density and ionization fraction rise. Above some threshold, electrons will ionize too many neutrals and the ionization rate will begin to decrease because of the reduced neutral density. As a result, the electron density will subsequently decrease. Although this physical interpretation is common in the literature, it has yet to be confirmed numerically, analytically, or experimentally. Indeed recent studies have shown that the formation of these oscillations may be more nuanced than this simple picture.

As a notable example, one recent numerical model shows that including an equation allowing the IAT wave energy to propagate can lead to large plasma potential, density, and temperature fluctuations in the plasma plume at low frequency.[12, 14] These numerical results are similar to experimental measurements of these low-frequency plasma oscillations.[9, 10] Through this numerical model Sary et. al. have proposed the following mechanism for the instability: Assuming the electron Mach number is sufficiently high to onset IAT, the wave energy can grow and lead to electron heating. The growth of the IAT quenches itself through electron Landau damping and this region of high plasma density propagates out of the cathode at the IAT group velocity. Experimental measurements have shown that these low frequency modes indeed propagate near the IAT group velocity.[15] However, this evidence is insufficient to support this theory over the predator-prey model. This is because ionization waves likely also propagate near the ion sound or drift speed. Furthermore, other numerical models that also include the same effects from plasma turbulence do not resolve any large scale plasma oscillations.[3]

Despite this promising and on-going work, there appear to be several points of contention in the literature as to the nature of this instability. What is the energy source for the instability? Is a zero-dimensional model sufficient or is there spatial dependence? Is a linear analysis sufficient to describe its behavior? What is the onset criterion? What drives the observed frequency and wavelength? Is there an interaction between this mode and the IAT? Given these outstanding questions and conflicting interpretation surrounding the nature of this mode, there is an apparent need for further experimental measurements and theoretical understanding of these low frequency oscillations. In this article, we begin with an experimental investigation into the modes. We then interpret these results through some analytical theory. This lends itself to a physical picture for the propagation of these low frequency structures.

2 EXPERIMENTAL AND ANALYSIS TECHNIQUES

To answer some of these outstanding questions, we measure the spatial variation of the propagation characteristics of the instabilities in the cath-

ode plume. Additionally we identify the relationship, if any, between the IAT and the observed low-frequency structures. To this end we first describe the experimental apparatus including the facility, cathode, and probes. This is followed by a discussion of the techniques used in our analysis.

2.1 Apparatus

The experiments were conducted in NASA Glenn Research Center's (GRC) Vacuum Facility-56, which is 3 ft in diameter and 4 ft long. The facility is pumped by an cryogenic pump and achieves base pressures of 0.1 μTorr. The pressure was monitored using an ionization gauge. The pressure in the facility was between $40-60$ μTorr-Xe during operation.

The BaO hollow cathode used for this experiment was designed for a nominal operating current of 20 A and was operated using 99.999% Xe gas. The propellant flow to the cathode was varied from 10 to 14 sccm. Only the condition at 10 sccm was in plume mode, with large low-frequency oscillations. A discharge filter was used to prevent interactions between the power supply and the plasma. The current to the cathode was controlled to 23 A during the experiment. The discharge anode was mounted at a distance of 38 mm from the keeper face. This anode was made of tungsten with a water-cooled copper solenoid, though this solenoid was not in use during this experiment. The discharge parameters were recorded using the facility's data acquisition and control system.

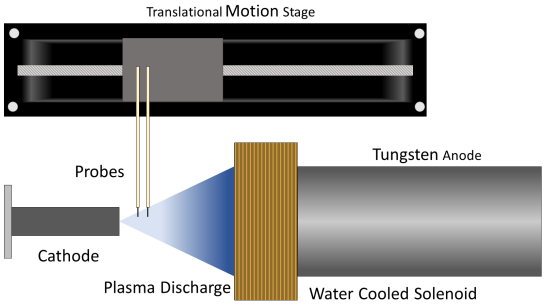

Figure 1: Experimental setup for probe measurements of low frequency plasma waves in a hollow cathode discharge. The setup is viewed from above.

Fluctuations in the ion saturation current were measured using two Langmuir probes, approximately 2 mm in length and 0.5 mm in diameter and spaced by 5 mm. The Langmuir probe was biased to -30 V to measure the ion saturation current. The probes were moved axially between the cathode and the anode by a linear motion stage. The ion saturation current was measured using an oscilloscope acquiring at 10 MHz at positions between the anode and the cathode in 1 mm increments. The experimental setup is illustrated in Fig. 1.

2.2 Analysis Techniques

From cylindrical Langmuir probe theory, the current collected by an ion saturation probe is

$$i_{sat} = 0.61 q A_p \sqrt{\frac{T_e}{m_i}} n, \tag{1}$$

where q is the unit charge, A_p is the probe area, T_e is the electron temperature, m_i is the ion mass, and n is the plasma density. If we assume that temperature fluctuations are slow compared to those in density, then the relationship

$$\frac{\delta i_{sat}}{\bar{i}_{sat}} = \frac{\delta n}{n_0}\ , \tag{2}$$

is the is established. In Eqn. 2, δi_{sat} and δn are the fluctuations in ion saturation current and plasma density, respectively and $\bar{i}_{sat}$ and n_0 are the steady state ion saturation current and plasma density. This relationship is used to determine the relative fluctuation in the plasma density.

We primarily use two techniques to interpret the experimental measurements of these plasma density fluctuations. To understand how the modes in the cathode plume evolve in time, we use a continuous wavelet transform for time-frequency analysis of the ion current fluctuations [16]. The continuous wavelet transform is defined as

$$\chi(\omega,\tau) = \sqrt{\omega}\int_{-\infty}^{\infty} x(t)\bar{\psi}\left(\omega\left(t-\tau\right)\right)dt\ , \tag{3}$$

where $\chi(\omega,\tau)$ is the amplitude of the wavelet at time τ with frequency ω and $\bar{\psi}(t)$ is the wavelet function. Typically wavelets are of the form $\bar{\psi}(t) = w(t)e^{it}$, where $w(t)$ describes the temporal extent of wavelet. We have have used a generalized Morse wavelet in our analysis.[17] Additionally, we

use the measured signals to estimate the dispersion of the plasma, $D(\omega, k) = 0$, with the Beall technique.[18] With this technique, we can identify the modes in the plasma as well as their propagation characteristics. Of particular interest is the phase velocity, which is calculated as

$$v_{ph} = \frac{\omega}{k}\ , \tag{4}$$

where ω is the frequency and k is the wavenumber of the dominant mode in the plasma. Here, k indicates the direction of propagation of a mode. When $k < 0$, the mode propagates towards the cathode while $k > 0$ is propagation towards the anode.

3 RESULTS

We discuss in this section the results from our analysis of the fluctuations in the cathode plasma. We first examine the transient behavior of the modes in the plasma using wavelet analysis and then identify them by estimating the dispersion. Next, we study the spatial structure of the propagating modes. These results are then compared to analytical theory. Since flow rates above 10 sccm did not exhibit the low-frequency waves we are interested in understanding, we focus our analysis on the 10 sccm condition. By reducing the flow rate from 12 sccm to 10 sccm, the low-frequency structures appeared in the discharge and the plume mode onset.

3.1 Wavelet Analysis and Dispersion Relations

Figure 2 shows the result of the wavelet analysis of the ion saturation probe signal. As has been reported before, we observe two modes, a low frequency oscillation near 40 kHz and higher frequency oscillations at frequencies above 200 kHz. Figure 2 indicates that while the amplitude of the low-frequency oscillations is time invariant, the higher frequency modes are not. In fact, the high frequency modes manifest themselves as periodic bursts rather than consistent oscillations. Not only does the amplitude of the high frequency modes oscillate, but its frequency is equal to that of the low-frequency oscillation. This transient behavior is consistent with the description provided by Sary et. al, where high frequency acoustic waves grow and saturate in the cathode plume leading to low frequency density fluctuations.

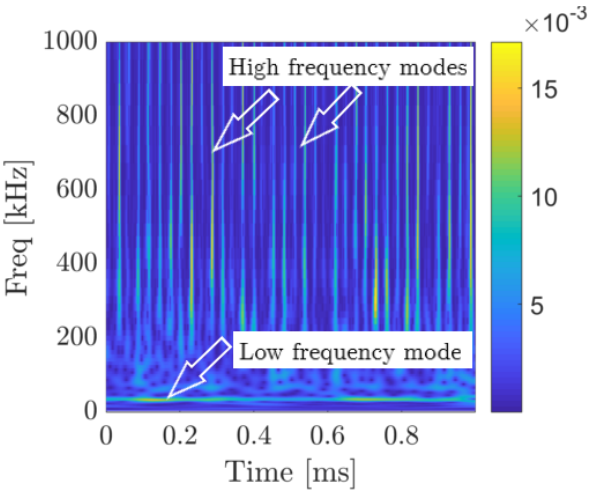

Figure 2: A representative example of the output of the wavelet analysis. The color axis is $\chi(\omega, \tau)$ from Eqn. 5. The amplitude of the modes above 200 kHz fluctuates in time at about 40 kHz.

Now, we can identify the modes in the plasma by estimating the dispersion using the Beall technique. Figure 3 shows the oscillation frequency against the wavevector. The intensity is proportional to the amplitude of the wave at that frequency wavelength. All together, this plot shows the amplitude of the modes that propagate in the plasma. Figure 3 shows the dispersion at three positions in the cathode plume. We find that the low frequency modes that are traditionally associated with predator-prey ionization waves have well defined wavelengths and frequencies. The higher frequency waves exist in a broad range of wavelengths and frequencies and have been observed before by Jorns et. al..[1] Our novel observation is that their amplitude appears to be fluctuating in time.

Furthermore, Figs. 3a-3c, indicate that the dominant modes change with location in the discharge. Figure 3a shows the dispersion at $z = 1$ mm. At this location we observe a 40 kHz oscillation that is propagating towards the cathode, $k < 0$ as well as some turbulent ion acoustic modes that also appear to propagate backwards. Figure 3b shows

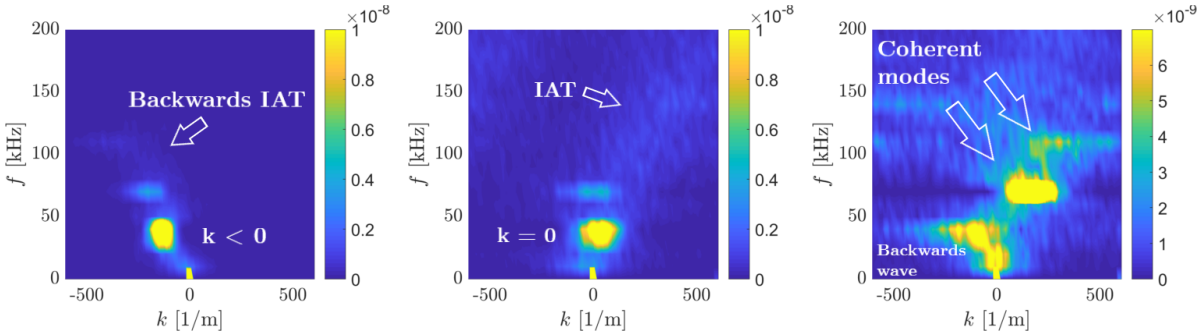

(a) The measured dispersion relation as at $z = 1$ mm. Here we observe a wave that propagates towards the cathode.

(b) The measured dispersion relation as at $z = 10$ mm. At this position $k = 0$, implying that the plasma between the probes is oscillating in phase.

(c) The measured dispersion relation as at $z = 21$ mm. Two coherent modes are present in the plasma as well as the wave propagating towards the cathode.

Figure 3: Dispersion measurements at various positions in the cathode plume. Figures are saturated to show detail.

Table 1: calculated phase velocities of the measured dispersion relations in Fig. 3.

z [mm]	v_{ph} [m/s]
1	-2400
10	$-$
21	$-2300,\ 2300,\ 2600$

the dispersion at $z = 10$ mm. At this position, the wavevector of the 40 kHz oscillation has shifted to $k = 0$. This implies that the plasma between the two probes is oscillating in phase. Additionally, there exist some turbulent ion acoustic modes in the plasma. These modes are of relatively small amplitude compared to the low-frequency wave. Figure 3c show the measured dispersion at $z = 21$ mm. Here, we observe several modes in the plasma. First, there exist two coherent modes that propagate towards the anode. These modes appear to travel at slightly different phase velocities. Second, a wave that propagates towards the cathode reappears.

The wavelet analysis and the measured dispersion relations suggest the following physical picture. The amplitude of the ion acoustic like modes are oscillating in time at a frequency equal to that of the low-frequency mode. The region where $k \simeq 0$ can be interpreted as a point source for the instability. Figures 3a-3c suggest that the waves originate from a point source and propagate away. We further explore this hypothesis in the following section by examining the spatial propagation of these modes.

3.2 Spatial Structure of Propagating Modes

Now that we have established the coexistence of the coherent, low-frequency modes and IAT, we will more closely examine the spatial dependence of these modes. The signal captured by the oscilloscope is clouded in noise. To better observe the low-frequency propagating structures in both the plasma density and in the IAT, we must average the signal from the ion saturation probe. Below, we discuss the averaging technique used in our analysis and present the results.

Figure 4 shows the continuous wavelet transform of the signal captured from the ion saturation probes at two points in time, separated by about 2.5 μs. The amplitude of the IAT modes changes in time while the amplitude of the low-frequency modes is time invariant. In our analysis, we find that the low-frequency modes oscillate at frequencies below 200 kHz. To discriminate between the low-frequency modes and the IAT modes, we use a cut-off frequency of 200 kHz in our analysis of the IAT.

We can estimate the total energy density in the IAT as a function of time by integrating from the

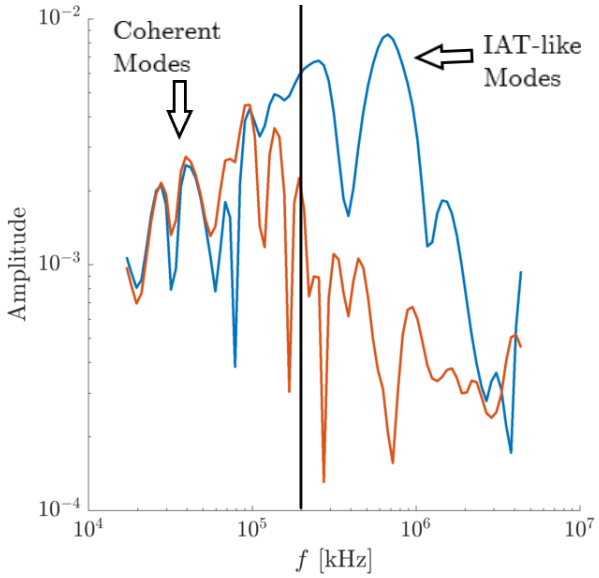

Figure 4: Comparison of the frequency spectra resulting from the wavelet analysis at different times within a cycle. The amplitude of the IAT-like modes changes in time, while the coherent modes do not. The vertical line denotes the 200 kHz cutoff for the IAT-like modes.

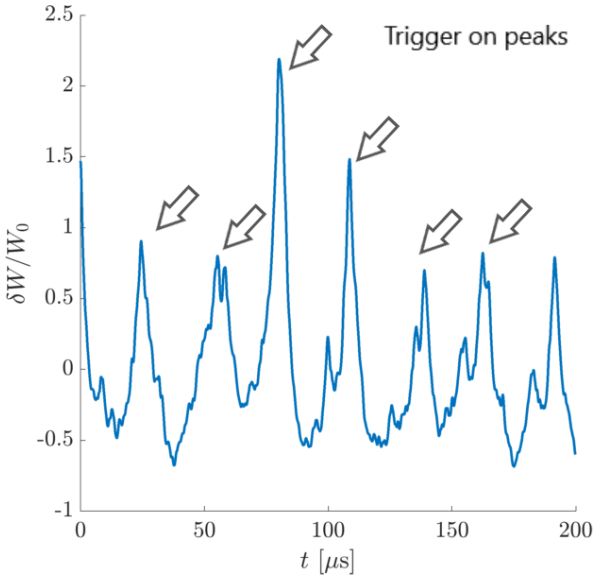

Figure 5: Relative fluctuations in wave energy density. The peaks in this trace are used to trigger the average.

cut-off frequency, ω_1, to the highest frequency in the measured spectrum, ω_2,

$$W(\tau) \propto \int_{\omega_1}^{\omega_2} \chi^2(\omega, \tau) d\omega \, . \tag{5}$$

From Eqn. 5, we can calculate the relative fluctuation in wave energy density, $\delta W/W_0$ as a function of time. A representative output of this calculation is shown in Fig. 5. Using the maxima of the IAT wave energy ($\max(\delta W/W_0)$) as a trigger, shown in Fig. 5, we then compute a triggered average of the wave energy density showing a few cycles. The average the plasma density fluctuation is calculated using the peaks in Fig. 5 as a trigger and averaging the raw measurement from the ion saturation probe, showing a few cycles of oscillation. We compute these averages at all positions in the plume. Note that the resulting waveforms are not correlated in time.

Figure 6 shows the results of the triggered average analysis. We observe clear coherent structures forming in both the plasma density and IAT wave energy density. Figure 6a shows two cycles of the oscillation at $z = 1$ mm. A quasi-sinusoidal oscillation in the plasma density is observed, while the fluctuation in the wave energy density is periodic but nonlinear. The frequency of oscillation for both the ion and wave energy densities is 40 kHz. Figure 6b shows the same fluctuations at 15 mm. At this position, two coherent density structures begin to form. The IAT wave energy density fluctuation has decreased, however its shape does not qualitatively change like the density. Lastly, Fig. 6c shows these oscillations at $z = 21$ mm. At this location the coherent structures are now distinct and the IAT perturbation continues to retain its shape. The period of fluctuation in the IAT wave energy density is exactly that of the low-frequency waves. Furthermore, there is a developing phase relationship between the IAT energy and the plasma density fluctuation that changes as a function of position. Near the cathode, the IAT energy leads the density fluctuation. Downstream, the density fluctuation leads the IAT energy.

The evidence in Figs. 3 and 6 both help create the physical picture that a point source in the plume generates structures in both the plasma density and IAT wave energy that propagate away from that location. The structures that propagate

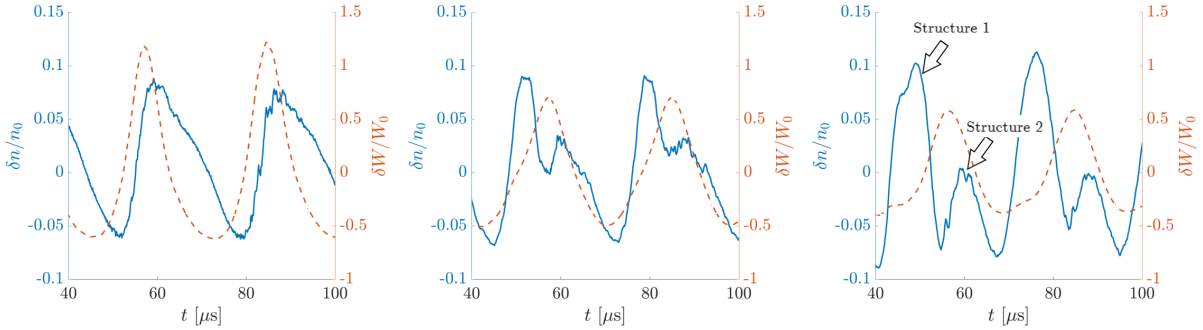

(a) Quasi-sinusoidal plasma density and IAT wave energy density waves are observed at $z = 1$ mm. The frequency of oscillation is 40 kHz.

(b) Two coherent density structures begin to separate and propagate at $z = 15$ mm. The IAT wave energy density continues to oscillate quasi-sinusoidally with a reduced amplitude.

(c) Two coherent structures are propagating at $z = 21$ mm. The IAT wave energy density continues to oscillate quasi-sinusoidally with a reduced amplitude.

Figure 6: Two cycles of the waveform captured by the ion saturation probe at three locations in the cathode plume. The cathode was at the 23 A, 10 sccm condition. Note, each position is measured at a different time. The measurements at each position are not correlated in time.

towards the anode appear to break up into distinct perturbations, while those that propagate towards the cathode remain quasi-periodic. The coexistence of low-frequency coherent modes with turbulent acoustic modes has been observed in the literature and is discussed further in the following section. [19]

4 DISCUSSION

To interpret these trends, we note that previous studies have shown that similar types of coherent structures propagating concurrently with IAT energy. In these works, the large scale oscillations are termed “solitons."[19] Ion acoustic solitons are nonlinear and coherent plasma structures that qualitatively share many properties with the low-frequency fluctuations we have measured in the cathode plume. Solitons propagate in a plasma near the ion acoustic speed, they are coherent, and can be periodically excited.[20] In this section, we first review the relevant theory of ion acoustic solitons. We then interpret our experimental measurements through the lens of this analytical theory.

4.1 Theory for Low-Frequency Modes

In a departure with previous linear perturbation analyses of the cathode plume [13, 15], we propose that the generation of ion acoustic solitons may be the source of coherent, low-frequency oscillations. Ion acoustic solitons are coherent plasma oscillations born out of a balance between the nonlinearity of convection and wave dispersion. These waves have been studied extensively both experimentally and theoretically since the 1960’s in double plasma devices.[21–24] Furthermore, solitons are known to exist in a dynamic equilibrium with ion acoustic turbulence, which has been measured in the cathode plume.

The waveform for solitons can be derived from the fluid equations for ions and electrons and Poisson’s equation. In the ion frame of reference, the ion continuity and momentum equations are

$$\frac{\partial n_i}{\partial t} + \frac{\partial n_i u_i}{\partial x} = 0 \,, \tag{6}$$

$$\frac{\partial u_i}{\partial t} + u_i \frac{\partial u_i}{\partial x} = -\frac{\partial \Phi}{\partial x} \,. \tag{7}$$

Here, we have neglected ionization and assumed the ions are cold. For the electrons, we assume that the electron mass is negligible such that the

electron momentum equation is simplified to:

$$n_e \frac{\partial \Phi}{\partial x} + \frac{\partial n_e}{\partial x} = 0 \ , \tag{8}$$

and Poisson's equation is simply:

$$\frac{\partial^2 \Phi}{\partial x^2} = n_i - n_e \ . \tag{9}$$

In Eqns. 6 - 9, $n_{i(e)}$, u_i, Φ are the ion (electron) density, velocity and electric potential, respectively. The densities are normalized by their steady state quantities, the velocities by the ion sound speed, $c_s = \sqrt{qT_e/m_i}$, the length by the Debye length and the potential by the electron temperature. Following the procedure of Washimi and Tanuiti [21], it can be shown that the fluctuation in electron density is given by [21, 22, 25]

$$\frac{\partial n_e^{(1)}}{\partial \tau} + n_e^{(1)} \frac{\partial n_e^{(1)}}{\partial \xi} + \frac{1}{2} \frac{\partial^3 n_e^{(1)}}{\partial \xi^3} = 0 \ . \tag{10}$$

This is the well known Korteweg De-Vries equation for ion acoustic waves.[26] From Eqn. 10, we see that the rate of change of the density is balanced between the nonlinearity of convection (the second term) and dispersion (third term). The stationary solution to this problem is the so-called solitary wave, or soliton, and is given by

$$n(x,t) = \delta n \, \mathrm{sech}^2 \left(\frac{x - u\,t}{D} \right) \ , \tag{11}$$

where we have dropped $n_e^{(1)}$ in favor of n. In this equation, δn is the amplitude of the soliton, u is the soliton speed, and D is its width. The following relationships between δn and the other parameters are

$$\left(\frac{D}{\lambda_D} \right)^2 = 6 \frac{n_0}{\delta n} \ , \tag{12}$$

$$u = c_s \left(1 + \frac{1}{3} \frac{\delta n}{n_0} \right) \ , \tag{13}$$

where n_0 is the steady state plasma density. From Eqns. 12 and 13, we find that as the amplitude of the wave increases, the width decreases and the speed of propagation increases. Conducting a Galilean transform to the laboratory frame, we find that Eqn. 13 becomes

$$u = c_s \left(1 + \frac{1}{3} \frac{\delta n}{n_0} \right) + u_i \ , \tag{14}$$

where u_i is the ion drift velocity. This theory, is in agreement with our current understanding of the low-frequency modes in the cathode plume. It is coherent, and propagates near the ion acoustic speed. If supported by experiment, this analytical theory allows us to answer some key questions about mode including the propagating characteristics, spatial dependence of the structure, and the sufficiency of a zero-dimensional model and of a linear analysis. The following is a comparison of this analytical theory with the experimental results provided in Sec. 3

4.2 Comparison of Experimental Results to Analytical Theory

Taking a closer look at $z = 21$ mm, we have curve fit the density fluctuation using Eqn. 11 with $\delta n/n_0$ and $\tau = (D/u)$ as free fit parameters; where we have interpreted each peak in the time series as an individual soliton. Figure 7 shows the result of the curve fit over three cycles of oscillation. We find good qualitative agreement between the experimental measurements and Eqn. 11. The average height and width of the three structures in our waveform are shown in Table 2. We similarly estimate the phase velocity of each soliton at $z = 21$ mm by identifying them as the coherent structures in the dispersion measurements of Fig. 3c. These estimates are also shown in Table 2.

Table 2: The average amplitude, δn, and temporal width, τ, of the waveform as found by a curve fit of the data at $z = 21$ [mm] to Eqn. 11. The phase velocity, u, is found from the estimated dispersion.

Soliton	$\delta n/n_0$	τ [μs]	u [m/s]
1	0.27 ± 0.01	5.8 ± 0.1	2600 ± 700
2	0.143 ± 0.004	5.0 ± 0.9	2300 ± 600

Without measurements of the electron temperature and the plasma density, we cannot conduct an absolute comparison of these fit parameters to the theory (Eqn. 11); however we can compare the ratio of average height-to-width under the assumption that the waveform consists of two solitons. Manipulating Eqn. 12 we see that for two

Table 3: Comparison of the speed and width of the soliton to those predicted by the theory and measured amplitude for solitons 1 and 2.

	$\frac{D_1}{D_2}$	u_1 $[m/s]$	u_2 $[m/s]$	D_1 $[\mu m]$	D_2 $[\mu m]$
Predicted	0.73 ± 0.2	2650 ± 700	2570 ± 700	20 ± 5	27 ± 6
Measured	1.3 ± 0.6	2600 ± 700	2300 ± 600	15000 ± 3000	12000 ± 2400

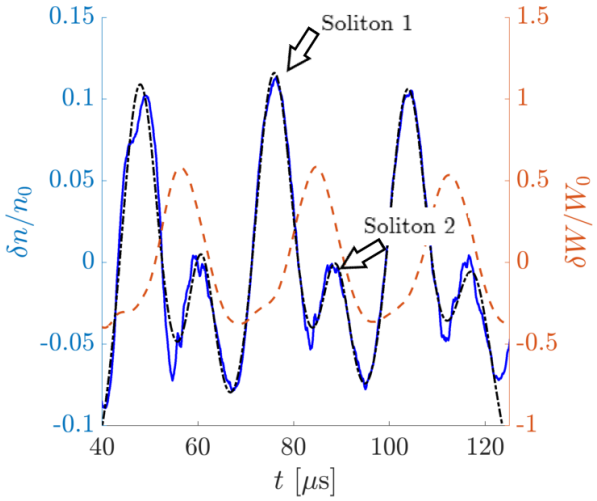

Figure 7: Three cycles of the ion density fluctuation, in blue, at $z = 21$ mm are shown. The curve fit using Eqn. 11 is in black. The wave energy density fluctuation is in red.

solitons

$$\frac{D_1}{D_2} = \frac{\tau_1 u_1}{\tau_2 u_2} = \sqrt{\frac{\delta n_2}{\delta n_1}} \,. \tag{15}$$

Using the results from Table 2 we find that, within the uncertainty of the experiment, the width-to-amplitude ratio of the measured waves in the cathode plume is in agreement with soliton theory. The results of this calculation is shown in Table 3. The uncertainty is primarily driven by our technique for determining the wave speed, which we have determined from the HWHM of the dispersion amplitude along the k axis of the Fig. 3c. As further evidence that these structures may be described as solitons, we can compare the inferred phase velocities for the soliton-like structures to the result of Eqn. 14. From the literature[1], we know that ion acoustic waves with a group velocity of $v_g = u_i + c_s$. This relationship allows us to rewrite Eqn. 14 as

$$u = v_g + c_s \left(\frac{1}{3} \frac{\delta n}{n_0} \right) \,. \tag{16}$$

To calculate the right hand side of this equation, we need estimates of the IAT group velocity and the ion sound speed. We can estimate the IAT group velocity by curve fitting the dispersion above 200 kHz. The measured IAT group velocity is 2500 ± 700 m/s. If we assume the electron temperature as 3 eV (typical for most cathodes), we find $c_s \simeq 1500$ m/s. Table 3 shows the results of this calculation. We find that the theoretical results are within uncertainty of the measured phase velocities for solitons 1 and 2. The uncertainty in v_g, however, is large compared to $c_s \left(\frac{1}{3} \frac{\delta n}{n_0} \right)$.

Although certain key features seem in line with soliton theory, there is at least one feature in stark disagreement. We can also test Eqn. 12 directly by assuming that a steady state plasma density of $n_0 = 10^{-19}$ m^{-3}.[1] Now the Debye length of the plasma is known and D can be calculated, in terms of the soliton amplitude. The result of this calculation for solitons 1 and 2 is shown in Table 3. The observed widths are calculated from the fit results in Table 2 and are also shown in Table 3. The structures we observe are $D \sim 10,000\,\lambda_D$, where as the solitons predicted by the theory and observed in the literature are $D \sim 10\,\lambda_D$. The reason for this discrepancy is not known and in part works against our interpretation of these structures as solitons. There could be a few potential explanations. A possible reason for this discrepancy between theory and experiment could be related to the relaxation time of the perturbation to a soliton waveform. An initial disturbance of arbitrary form can relax to the soliton state. It is possible that in our measurements the initial perturbation is broader than a soliton and there has been insufficient time for the waveform to have completely relaxed to the soliton state, resulting in a wider struc-

ture. Another possibility is related to the simplifying assumptions. For example, ionization was not considered in the theoretical development but could be altering the density profile on similar timescales as the fluctuations in the plasma. Although the width of the structure is underestimated by a soliton description, the theory is still able to capture many of the properties of these low-frequency oscillations.

Having discussed the density perturbations, we now pivot our discussion to the IAT wave energy density fluctuations. The total energy in the turbulent modes fluctuates in time with its own soliton-like structure, shown in Figs. 6a-6c. Similarly curve fitting the averaged waveform in Fig. 7 to Eqn. 11, we find the temporal width $\tau = 6.3 \pm 0.2$ μs and an amplitude of $\delta W/W_0 = 1.08 \pm 0.02$. The width of the IAT energy oscillation is similar to that of soliton 1, while its amplitude is three times larger than the density perturbation (noting the different scales in Fig. 7). As was observed in Figs. 6a-6c these bursts of turbulent energy propagate with a developing phase relationship with the density pertrubation. In the literature similar characteristics have been observed when locally exciting a plasma. When the plasma is perturbed, IAT is generated as a wave packet and it propagates away from the source.[27, 28] It is possible that this process occurs in the cathode plume.

5 PHYSICAL SIGNIFICANCE

In light of the results presented above, we return to the outstanding questions about the coherent structures in cathode plumes outlined Sec. 1:

1. *Is a linear analysis sufficient?* The weakly-nonlinear theory for solitary waves is shown to be in relatively good agreement with experiment (with some exceptions), indicating that a linear theory may be insufficient to describe the evolution of the mode.

2. *Is a zero-dimensional model sufficient or is there spatial dependence?* The waveforms and dispersion are both changing spatially and appear to indicate that there is a localized "source" of the instability. Periodic impulses disperse energy to several types of waves that propagate away from this location in the plume. This type of behavior cannot be captured by a zero-dimensional model.

3. *Is there an interaction between this mode and the IAT?* We have observed an oscillation in the IAT wave energy density that appears to propagate away from the "source" and has the same period as the density fluctuation. IAT energy density fluctuations are clearly correlated, however these measurements do not necessarily indicate that they are related to the generation of the low-frequency waves.

Our theory and measurements create a physical picture where a localized and periodic disturbance in the plasma generates the instabilities. The energy in this "source" region is dispersed into several modes: IAT and coherent low-frequency structures that propagate towards the anode and a quasi-periodic wave propagating towards the cathode. The IAT is generated periodically similar to a wave packet. The low-frequency, anode propagating structures are, for the most part, well described by soliton theory. The wave that propagates to the cathode could contribute to the enhanced erosion observed when the cathode is operating in plume mode. This new understanding of how the mode evolves will lead to future experimental and theoretical investigations into the origin of these waves.

6 CONCLUSIONS

Ion saturation probes have been used to measure the spatial dependence of waves present in a hollow cathode operating in the plume mode. These measurements indicate that localized, periodic impulses near the cathode are the source of the instabilities in the plasma. The energy in the "source" region disperses into IAT and coherent, low-frequency waves that propagate towards the anode as well as a quasi-periodic wave that propagates towards the cathode. The low-frequency anode propagating modes are interpreted with a weakly nonlinear formulation of ion acoustic solitons. The measured height-to-width ratio and velocity of the wave are in good agreement with the theory, however observed width is four orders of magnitude larger than predicted. In addition to these density perturbations, we have measured an oscillation in the total IAT energy through wavelet

analysis and averaging. The total energy of these turbulent modes fluctuates in time with an evolving phase relationship with the low-frequency density perturbations. The IAT appears to be generated and propagate like a wave packet in the cathode plume. This collection of new experimental evidence has created a new picture for the evolution of the waves associated with the cathode plume mode, where plasma instabilities are generated from a localized source in the plume.

7 ACKNOWLEDGEMENTS

This work was supported by the NASA Space Technology Research Fellowship under the grant number NNX15AQ37H. The authors would like to thank Tim Sarver-Verhey and the facility technicians at NASA Glenn Research Center for the use of their vacuum facility, cathode and anode for the experiments.

REFERENCES

[1] Jorns, B. A., Dodson, C., Goebel, D. M., and Wirz, R., "Propagation of Ion Acoustic Wave Energy in the Plume of a High-Current LaB6 Hollow Cathode," *Physical Review E*, Vol. 96, No. 2, Aug. 2017, pp. 023208.

[2] Mikellides, I. G., Katz, I., Goebel, D. M., and Jameson, K. K., "Evidence of Nonclassical Plasma Transport in Hollow Cathodes for Electric Propulsion," *Journal of Applied Physics*, Vol. 101, No. 6, March 2007, pp. 063301.

[3] Lopez Ortega, A., Mikellides, I. G., and Jorns, B., "First-Principles Modeling of the IAT-Driven Anomalous Resistivity in Hollow Cathode Discharges II: Numerical Simulations and Comparison with Measurements," American Institute of Aeronautics and Astronautics, July 2016.

[4] Csiky, G. A., "Measurements of Some Properties of a Discharge from a Hollow Cathode," *NASA Technical Note*, 1969.

[5] Philip, C., "A Study of Hollow Cathode Discharge Characteristics," *AIAA Journal*, Vol. 9, No. 11, Nov. 1971, pp. 2191–2196.

[6] Domonkos, M. T., Gallimore, A. D., Williams Jr, G. J., and Patterson, M. J., "Low-Current Hollow Cathode Evaluation," *Joint Propulsion Conference*, No. 2575, American Institute of Aeronautics and Astronautics, Los Angeles, CA, 1999, p. 48109.

[7] Williams, G.J., J., Smith, T., Domonkos, M., Gallimore, A., and Drake, R., "Laser-Induced Fluorescence Characterization of Ions Emitted from Hollow Cathodes," *IEEE Transactions on Plasma Science*, Vol. 28, No. 5, Oct. 2000, pp. 1664–1675.

[8] Mikellides, I. G., Katz, I., Goebel, D. M., Jameson, K. K., and Polk, J. E., "Wear Mechanisms in Electron Sources for Ion Propulsion, II: Discharge Hollow Cathode," *Journal of Propulsion and Power*, Vol. 24, No. 4, 2008, pp. 866–879.

[9] Goebel, D. M., Jameson, K. K., Katz, I., and Mikellides, I. G., "Potential Fluctuations and Energetic Ion Production in Hollow Cathode Discharges," *Physics of Plasmas (1994-present)*, Vol. 14, No. 10, Oct. 2007, pp. 103508.

[10] Georgin, M. P., Byrne, M., Jorns, B. A., and Gallimore, A., "Passive High-Speed Imaging of Ion Acoustic Turbulence in a Hollow Cathode," *53rd AIAA/SAE/ASEE Joint Propulsion Conference*, No. 4973, American Institute of Aeronautics and Astronautics, 2017.

[11] Mandell, M. and Katz, I., "Theory of Hollow Operation in Spot and Plume Modes," American Institute of Aeronautics and Astronautics, June 1994.

[12] Sary, G., Garrigues, L., and Boeuf, J.-P., "Hollow Cathode Modeling: II. Physical Analysis and Parametric Study," *Plasma Sources Science and Technology*, Vol. 26, No. 5, 2017, pp. 055008.

[13] Fife, J., Martinez-Sanchez, M., and Szabo, J., "A Numerical Study of Low-Frequency Discharge Oscillations in Hall Thrusters," American Institute of Aeronautics and Astronautics, July 1997.

[14] Sary, G., Garrigues, L., and Boeuf, J.-P., "Hollow Cathode Modeling: I. A Coupled Plasma Thermal Two-Dimensional Model," *Plasma Sources Science and Technology*, Vol. 26, No. 5, 2017, pp. 055007.

[15] Georgin, M. P., Jorns, B. A., and Gallimore, A. D., "An Experimental and Theoretical Study of Hollow Cathode Plume Mode Oscillations," Vol. IEPC-2017-298, Electric Rocket Propulsion Society, Atlanta Georgia, Oct. 2017.

[16] Grossmann, A. and Morlet, J., "Decomposition of Hardy Functions into Square Integrable Wavelets of Constant Shape," *SIAM Journal on Mathematical Analysis*, Vol. 15, No. 4, July 1984, pp. 723–736.

[17] Olhede, S. C. and Walden, A. T., "Generalized Morse Wavelets," *IEEE Transactions on Signal Processing*, Vol. 50, No. 11, Nov. 2002, pp. 2661–2670.

[18] Beall, J. M., Kim, Y. C., and Powers, E. J., "Estimation of Wavenumber and Frequency Spectra Using Fixed Probe Pairs," *Journal of Applied Physics*, Vol. 53, No. 6, June 1982, pp. 3933–3940.

[19] Petrov, A. E., Sarksyan, K. A., Skvortsova, N. N., and Kharchev, N. K., "Observation of Nonlinear Coupling between Drift and Ion-Acoustic Oscillations in Low-Frequency Plasma Turbulence," *Plasma Physics Reports*, Vol. 27, No. 1, 2001, pp. 56–61.

[20] Ikezi, H., "Experiments on Ion Acoustic Solitary Waves," *The Physics of Fluids*, Vol. 16, No. 10, Oct. 1973, pp. 1668–1675.

[21] Washimi, H. and Taniuti, T., "Propagation of Ion-Acoustic Solitary Waves of Small Amplitude," *Physical Review Letters*, Vol. 17, No. 19, Nov. 1966, pp. 996–998.

[22] Tran, M. Q., "Ion Acoustic Solitons in a Plasma: A Review of Their Experimental Properties and Related Theories," *Physica Scripta*, Vol. 20, No. 3-4, 1979, pp. 317.

[23] Nakamura, Y., "Experiments on Ion-Acoustic Solitons in Plasmas Invited Review Article," *IEEE Transactions on Plasma Science*, Vol. 10, No. 3, Sept. 1982, pp. 180–195.

[24] Lonngren, K. E., "Ion Acoustic Soliton Experiments in a Plasma," *Optical and Quantum Electronics*, Vol. 30, No. 7-10, Oct. 1998, pp. 615–630.

[25] Ott, E. and Sudan, R. N., "Nonlinear Theory of Ion Acoustic Waves with Landau Damping," *The Physics of Fluids*, Vol. 12, No. 11, Nov. 1969, pp. 2388–2394.

[26] Korteweg, D. J., "On the Change of Form of Long Waves Advancing in a Rectangular Canal, and on a New Type of Long Stationary Waves," *Philos. Mag.*, Vol. 39, 1895, pp. 422.

[27] Joyce, G., Lonngren, K., Alexeff, I., and Jones, W. D., "Dispersion of Ion-Acoustic Waves," *The Physics of Fluids*, Vol. 12, No. 12, Dec. 1969, pp. 2592–2599.

[28] Hamza, A. M., "On the Development and Evolution of Nonlinear Ion Acoustic Wave Packets," *Ann. Geophys.*, Vol. 23, No. 6, Sept. 2005, pp. 2249–2257.